

DEVELOPMENT OF THE BASIC DYNAMICAL MODEL OF A SQUIRREL CAGE MOTOR

Michal Hajžman, Miroslav Byrtus, Vladimír Zeman*

This paper deals with the basic dynamical model of electromotor whose creation was motivated by problems of electromotor vibrations and its subsequent fatigue. The model is characterized by a flexible shaft with mounted packet of sheet metals that are equipped with parallel copper bars connected by end shortcircuit rings. Finite element analysis is used for the discretization of the shaft, while the sheet metal packet of cylindrical shape is modelled as a set of rigid bodies joined using chosen viscoelastic forces and torques. The shortcircuit rings are supposed to be rigid in this basic dynamical model and the pieces of copper bars are substituted by massless springs of calculated properties. Problematic model parameters are identified by means of performed experimental modal analysis.

Keywords: squirrel cage motor, rotor dynamics, finite element method, modal analysis, parameter tuning

1. Introduction

One of the very interesting examples of rotating systems is a squirrel cage induction motor that is employed in various machines and means of transport mainly as a traction motor. The usage of this type of motor in vehicles is connected with possible fatigue problems because of non-stationary loading and changing operational conditions. General methods of mechanical system dynamics are suitable approaches to the mathematical modelling of a rotating part (Figure 1) of a squirrel cage motor. However very simple models (e.g. [1], [3]) are usually used for the dynamical analysis of this type of motors. The presented paper aims at the development of a more advanced and usable dynamical model.

The structure of the rotor of this studied type of an electric motor is shown in Figure 2. The rotor consists of a rotor shaft with laminated iron armature mounted in the middle shaft part. Laminations have the form of thin sheet metals with holes. The squirrel cage is composed of rotor bars (usually made of copper) that are put through the laminations and joined by end rings on both ends (also made of copper). The end rings can be constricted by shrink rings made of certain more stiff material. The short end pieces of rotor bars out of the armature are deformed during the rotor operation due to rings inertia and electromagnetic forces. Mentioned fatigue problems can be characterized by ruptures of the end ring and rotor bar connections. In order to investigate dynamical behaviour and dynamical properties of a rotor, the computational model was developed and is described in this paper. The model was created by theoretical way in general and the in-house software tool was implemented based on this development.

* Ing. M. Hajžman, Ph.D., Ing. M. Byrtus, Ph.D., prof. Ing. V. Zeman, DrSc., Department of Mechanics, University of West Bohemia in Pilsen; Univerzitní 8; 306 14 Plzeň

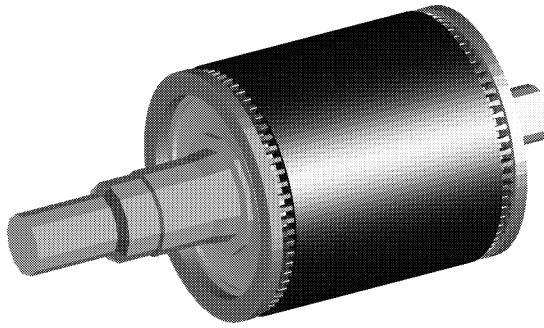


Fig.1: Rotor of a squirrel cage motor (visualization)

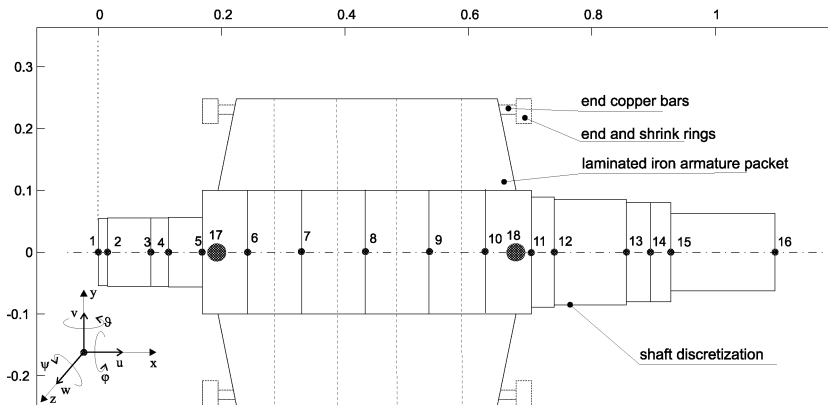


Fig.2: Scheme of the rotor of a squirrel cage motor

The model is called the basic dynamical model in which the end rings and shrink rings are considered as rigid bodies. It should be suitable for dynamical analyses with low-frequency excitation and motion. The basic dynamical model is composed of a flexible shaft modelled by means of 1D shaft finite elements, middle armature modelled as a set of five rigid bodies connected with translational and torsional springs, end parts of rotor bars modelled as massless discrete springs connecting the armature rigid bodies with end rings (considered together with shrink rings) rigid bodies.

2. Model of a rotor of a squirrel cage motor

The basic dynamical model of the rotor of the squirrel cage motor will be described in more detail in this section.

2.1. Flexible shaft model

The whole shaft of the motor (including the part with mounted sheet metal packet) is modelled as a flexible body by means of shaft finite elements derived e.g. in [2] or in [5] on the basis of Rayleigh theory (respecting rotary inertia). It is considered that the shaft has an undeformable cross-section that is still perpendicular to the deformed shaft centre-line. The shaft is discretized on 15 finite elements (see Figure 2) with 16 nodes (small dots with numbers in Figure 2). Motion of the shaft in each node is defined by three displacements (u , v , w) and three rotations (φ , ϑ , ψ). The mass, gyroscopic and stiffness

matrices $\mathbf{M}^{(e)} \in \mathbb{R}^{12,12}$, $\omega_0 \mathbf{G}^{(e)} \in \mathbb{R}^{12,12}$, $\mathbf{K}^{(e)} \in \mathbb{R}^{12,12}$ of the shaft element with nodes i and $i + 1$ are derived (see [2], [5]) for configuration space

$$\mathbf{q}^{(e)} = [u_i \ v_i \ w_i \ \varphi_i \ \vartheta_i \ \psi_i \ u_{i+1} \ v_{i+1} \ w_{i+1} \ \varphi_{i+1} \ \vartheta_{i+1} \ \psi_{i+1}]^T . \quad (1)$$

The vector of generalized coordinates of the whole shaft is

$$\mathbf{q}_R = [\mathbf{q}_1^T \ \mathbf{q}_2^T \ \dots \ \mathbf{q}_{16}^T]^T , \quad (2)$$

where \mathbf{q}_i , $i = 1, 2, \dots, 16$ are nodal vectors $\mathbf{q}_i = [u_i \ v_i \ w_i \ \varphi_i \ \vartheta_i \ \psi_i]^T$. Global mass matrix $\mathbf{M}_R \in \mathbb{R}^{96,96}$, gyroscopic effects matrix $\omega_0 \mathbf{G}_R \in \mathbb{R}^{96,96}$ and stiffness matrix $\mathbf{K}_R \in \mathbb{R}^{96,96}$ of the shaft are assembled using element matrices $\mathbf{M}^{(e)}$, $\omega_0 \mathbf{G}^{(e)}$, $\mathbf{K}^{(e)}$ with respect to the generalized coordinate vector (2). The global stiffness matrix can be extended by stiffness matrices of the bearings $\mathbf{K}_L^R \in \mathbb{R}^{6,6}$ and $\mathbf{K}_L^L \in \mathbb{R}^{6,6}$ on the positions corresponding to \mathbf{q}_3 and \mathbf{q}_{14} . A comprehensive approach to the roller-bearings modelling was presented in [6]. The conservative model of the flexible shaft is finally of the form

$$\mathbf{M}_R \ddot{\mathbf{q}}_R(t) + \omega_0 \mathbf{G}_R \dot{\mathbf{q}}_R(t) + \mathbf{K}_R \mathbf{q}_R(t) = \mathbf{0} , \quad (3)$$

where ω_0 is angular velocity of the rotor. Damping is not described in this paper, but it is easy to extend the model with the orthotropic damping of bearings, external isotropic environment damping and the internal material damping.

2.2. Laminated iron armature model

The whole laminated iron armature packet (composed of sheet metals with copper bars passing through) is mounted in the middle part of the shaft. It is modelled by a set of rigid bodies connected by flexible couplings that represent the influence of continuous copper bars inside the packet. Five rigid bodies (see Figure 2) are set in the shaft nodes 6 to 10. The mass matrices of particular rigid bodies are written as

$$\mathbf{M}_6 = \mathbf{M}_7 = \mathbf{M}_8 = \mathbf{M}_9 = \mathbf{M}_{10} = \text{diag}(m_D, m_D, m_D, I_{0D}, I_D, I_D) \quad (4)$$

and matrices of gyroscopic effects as

$$\omega_0 \mathbf{G}_6 = \omega_0 \mathbf{G}_7 = \omega_0 \mathbf{G}_8 = \omega_0 \mathbf{G}_9 = \omega_0 \mathbf{G}_{10} = \omega_0 \begin{bmatrix} 0 & 0 & 0 & 0 & 0 & 0 \\ 0 & 0 & 0 & 0 & 0 & 0 \\ 0 & 0 & 0 & 0 & 0 & 0 \\ 0 & 0 & 0 & 0 & 0 & 0 \\ 0 & 0 & 0 & 0 & 0 & I_{0D} \\ 0 & 0 & 0 & 0 & -I_{0D} & 0 \end{bmatrix} , \quad (5)$$

where m_D is the mass of one body and I_{0D} and I_D are its moments of inertia. The diagonal mass and block diagonal gyroscopic matrices of the whole laminated iron armature packet are

$$\mathbf{M}_D = \text{diag}(\mathbf{0}_1, \mathbf{0}_2, \dots, \mathbf{0}_5, \mathbf{M}_6, \mathbf{M}_7, \dots, \mathbf{M}_{10}, \mathbf{0}_{11}, \mathbf{0}_{12}, \dots, \mathbf{0}_{16}) , \quad (6)$$

$$\omega_0 \mathbf{G}_D = \omega_0 \text{diag}(\mathbf{0}_1, \mathbf{0}_2, \dots, \mathbf{0}_5, \mathbf{G}_6, \mathbf{G}_7, \dots, \mathbf{G}_{10}, \mathbf{0}_{11}, \mathbf{0}_{12}, \dots, \mathbf{0}_{16}) , \quad (7)$$

where $\mathbf{0}_i$ are square zero matrices of order 6.

In order to introduce the flexible behaviour between parts (rigid bodies) of discretized sheet metals packet resulting from the continuous cooper bars, it is necessary to develop also the stiffness matrix of the coupling between described rigid bodies. After simple derivation such stiffness matrix between two rigid bodies can be written as

$$\mathbf{K}_{C,D}^{i,i+1} = \left[\begin{array}{cccccc|cccccc} k_{ax} & 0 & 0 & 0 & 0 & 0 & -k_{ax} & 0 & 0 & 0 & 0 & 0 \\ 0 & 0 & 0 & 0 & 0 & 0 & 0 & 0 & 0 & 0 & 0 & 0 \\ 0 & 0 & 0 & 0 & 0 & 0 & 0 & 0 & 0 & 0 & 0 & 0 \\ 0 & 0 & 0 & k_t & 0 & 0 & 0 & 0 & 0 & -k_t & 0 & 0 \\ 0 & 0 & 0 & 0 & k_{oh} & 0 & 0 & 0 & 0 & 0 & -k_{oh} & 0 \\ 0 & 0 & 0 & 0 & 0 & k_{oh} & 0 & 0 & 0 & 0 & 0 & -k_{oh} \\ \hline -k_{ax} & 0 & 0 & 0 & 0 & 0 & k_{ax} & 0 & 0 & 0 & 0 & 0 \\ 0 & 0 & 0 & 0 & 0 & 0 & 0 & 0 & 0 & 0 & 0 & 0 \\ 0 & 0 & 0 & 0 & 0 & 0 & 0 & 0 & 0 & 0 & 0 & 0 \\ 0 & 0 & 0 & -k_t & 0 & 0 & 0 & 0 & 0 & k_t & 0 & 0 \\ 0 & 0 & 0 & 0 & -k_{oh} & 0 & 0 & 0 & 0 & 0 & k_{oh} & 0 \\ 0 & 0 & 0 & 0 & 0 & -k_{oh} & 0 & 0 & 0 & 0 & 0 & k_{oh} \end{array} \right], \quad (8)$$

where k_t is torsional coupling stiffness, k_{ax} is axial stiffness and k_{oh} is bending stiffness. Particular values of these stiffnesses can be estimated using elementary expressions of elasticity or they can be identified on the basis of certain measurement (as will be shown in next section of this paper). The whole stiffness matrix $\mathbf{K}_{C,D} \in \mathbb{R}^{96,96}$ of the discretized laminated iron armature package is composed of matrices $\mathbf{K}_{C,D}^{i,i+1}$ for $i = 6, 7, 8, 9$, placed as the submatrices on the positions corresponding to mounting nodes (see Figure 2).

2.3. Model of end and shrink rings

The end rings strengthened by shrink rings are connected with the copper bars ends in the outer sides of the rotor. Each set of end ring and shrink ring (on the left and on the right side) is considered as a rigid body with 6 degrees of freedom whose motion is described by 6 generalized coordinates. Therefore two new nodes (number 17 and 18) identical with ring gravity centres are added into the model (Figure 2). Their generalized coordinate vectors are

$$\mathbf{q}_{17} = [u_{17} \ v_{17} \ w_{17} \ \varphi_{17} \ \vartheta_{17} \ \psi_{17}]^T, \quad \mathbf{q}_{18} = [u_{18} \ v_{18} \ w_{18} \ \varphi_{18} \ \vartheta_{18} \ \psi_{18}]^T. \quad (9)$$

Mass and gyrosopic matrices of the rings are

$$\mathbf{M}_{PL} = \mathbf{M}_{PR} = \text{diag}(m_P, m_P, m_P, I_{0P}, I_P, I_P) \quad (10)$$

and

$$\omega_0 \mathbf{G}_{PL} = \omega_0 \mathbf{G}_{PR} = \omega_0 \left[\begin{array}{cccccc} 0 & 0 & 0 & 0 & 0 & 0 \\ 0 & 0 & 0 & 0 & 0 & 0 \\ 0 & 0 & 0 & 0 & 0 & 0 \\ 0 & 0 & 0 & 0 & 0 & 0 \\ 0 & 0 & 0 & 0 & 0 & I_{0P} \\ 0 & 0 & 0 & 0 & -I_{0P} & 0 \end{array} \right], \quad (11)$$

where m_P is the mass of the end ring (including shrink ring) and I_{0P} and I_P are corresponding moments of inertia.

2.4. Coupling of end rings and laminated armature packet

In order to connect end rings (including shrink rings) with the laminated iron armature packet the stiffness matrix representing free ends of copper bars should be developed. The couplings are considered massless and the appropriate end bar masses are added partly to the end rings and partly to the outer bodies of discretized sheet metal packet.

The end copper bars are characterized by translational stiffnesses k_ξ in axial direction, k_η in radial direction and k_ζ in tangential direction and analogical rotation stiffnesses $k_{\xi\xi}$, $k_{\eta\eta}$ and $k_{\zeta\zeta}$. Real values of these stiffnesses are the most problematic elements of the dynamic model because of the wear contact between the soft copper bars and sheet metal edges. The stiffness values can be either estimated or tuned on the basis of certain experimental data.

The compressed stiffness matrix of the i -th coupling (i -th end bar) on the left side is

$$\mathbf{K}_{i,L} = \begin{bmatrix} \tilde{\mathbf{K}}_{t_i} & \tilde{\mathbf{K}}_{t_i} \mathbf{R}_{i,L}^T & -\tilde{\mathbf{K}}_{t_i} & -\tilde{\mathbf{K}}_{t_i} \mathbf{R}_{i,17}^T \\ \mathbf{R}_{i,L} \tilde{\mathbf{K}}_{t_i} & \mathbf{R}_{i,L} \tilde{\mathbf{K}}_{t_i} \mathbf{R}_{i,L}^T + \tilde{\mathbf{K}}_{r_i} & -\mathbf{R}_{i,L} \tilde{\mathbf{K}}_{t_i} & -\mathbf{R}_{i,L} \tilde{\mathbf{K}}_{t_i} \mathbf{R}_{i,17}^T - \tilde{\mathbf{K}}_{r_i} \\ -\tilde{\mathbf{K}}_{t_i} & -\tilde{\mathbf{K}}_{t_i} \mathbf{R}_{i,L}^T & \tilde{\mathbf{K}}_{t_i} & \tilde{\mathbf{K}}_{t_i} \mathbf{R}_{i,17}^T \\ -\mathbf{R}_{i,17} \tilde{\mathbf{K}}_{t_i} & -\mathbf{R}_{i,17} \tilde{\mathbf{K}}_{t_i} \mathbf{R}_{i,L}^T - \tilde{\mathbf{K}}_{r_i} & \mathbf{R}_{i,17} \tilde{\mathbf{K}}_{t_i} & \mathbf{R}_{i,17} \tilde{\mathbf{K}}_{t_i} \mathbf{R}_{i,17}^T + \tilde{\mathbf{K}}_{r_i} \end{bmatrix} \in \mathbb{R}^{12,12}, \quad (12)$$

where matrices

$$\tilde{\mathbf{K}}_{t_i} = \begin{bmatrix} k_\xi & 0 & 0 \\ 0 & k_\eta C_i^2 + k_\zeta S_i^2 & k_\eta C_i S_i - k_\zeta S_i C_i \\ 0 & k_\eta C_i S_i - k_\zeta S_i C_i & k_\eta S_i^2 + k_\zeta C_i^2 \end{bmatrix}, \quad (13)$$

$$\tilde{\mathbf{K}}_{r_i} = \begin{bmatrix} k_{\xi\xi} & 0 & 0 \\ 0 & k_{\eta\eta} C_i^2 + k_{\zeta\zeta} S_i^2 & k_{\eta\eta} C_i S_i - k_{\zeta\zeta} S_i C_i \\ 0 & k_{\eta\eta} C_i S_i - k_{\zeta\zeta} S_i C_i & k_{\eta\eta} S_i^2 + k_{\zeta\zeta} C_i^2 \end{bmatrix} \quad (14)$$

are the local diagonal stiffness matrices of one end bar transformed into the global coordinate system rotated by angle β_i ($C_i = \cos \beta_i$, $S_i = \sin \beta_i$). Matrix

$$\mathbf{R}_{i,X} = \begin{bmatrix} 0 & -z_i & y_i \\ z_i & 0 & -x_i \\ -y_i & x_i & 0 \end{bmatrix}_X, \quad X = L, 17, \quad i = 1, 2, \dots, 62 \quad (15)$$

is composed of coupling point coordinates $[x_i, y_i, z_i]_X$ on the lamination packet ($\mathbf{R}_{i,L}$) and on the end ring ($\mathbf{R}_{i,17}$). Similar expressions hold also for the stiffness matrices $\mathbf{K}_{i,R}$ of right end bars.

The whole stiffness matrix $\mathbf{K}_V \in \mathbb{R}^{108,108}$ of all end copper bars is composed of described matrices $\mathbf{K}_{i,L}$ and $\mathbf{K}_{i,R}$ whose blocks are placed on the positions corresponding to generalized coordinate vectors \mathbf{q}_6 , \mathbf{q}_{10} , \mathbf{q}_{17} a \mathbf{q}_{18} .

2.5. Motion equations of the basic dynamical model of the electromotor rotor

After introduction of the global generalized coordinate vector of the whole rotor

$$\mathbf{q} = [\mathbf{q}_R^T \mathbf{q}_{17}^T \mathbf{q}_{18}^T]^T = [\mathbf{q}_1^T \mathbf{q}_2^T \dots \mathbf{q}_{16}^T \mathbf{q}_{17}^T \mathbf{q}_{18}^T]^T, \quad (16)$$

the basic dynamical model of the rotor of the squirrel cage motor is of the form

$$\begin{aligned} \begin{bmatrix} \mathbf{M}_R + \mathbf{M}_D & \mathbf{0} & \mathbf{0} \\ \mathbf{0} & \mathbf{M}_{PL} & \mathbf{0} \\ \mathbf{0} & \mathbf{0} & \mathbf{M}_{PR} \end{bmatrix} \ddot{\mathbf{q}}(t) + \omega_0 \begin{bmatrix} \mathbf{G}_R + \mathbf{G}_D & \mathbf{0} & \mathbf{0} \\ \mathbf{0} & \mathbf{G}_{PL} & \mathbf{0} \\ \mathbf{0} & \mathbf{0} & \mathbf{G}_{PR} \end{bmatrix} \dot{\mathbf{q}}(t) + \\ + \left(\begin{bmatrix} \mathbf{K}_R + \mathbf{K}_{C,D} & \mathbf{0} & \mathbf{0} \\ \mathbf{0} & \mathbf{0} & \mathbf{0} \\ \mathbf{0} & \mathbf{0} & \mathbf{0} \end{bmatrix} + \mathbf{K}_V \right) \mathbf{q}(t) = \mathbf{0}. \end{aligned} \quad (17)$$

Real parameter values were obtained using drawings and models from a motor producer and on the basis of additional calculations.

3. Tuning of the model parameters

The most problematic values of the rotor model parameters are the stiffnesses of end copper bars connecting the shortcircuit end rings with the laminated iron armature packet and the stiffness representing the flexible behaviour of the packet. The experimental modal analysis of the real rotor was performed (see [4]) and therefore the results can be used for the dynamic model parameter identification.

Optimization parameters for the parameter tuning problem are chosen as

$$\mathbf{p} = [p_1 \ p_2 \ p_3]^T, \quad (18)$$

while

$$p_1 = \frac{k_{T1}}{k_{T1,0}}, \quad p_2 = \frac{k_{T2}}{k_{T2,0}}, \quad (19)$$

where k_{T1} is torsional stiffness between parts 6 and 7 and parts 9 and 10 of the discretized sheet metal packet with continuous copper bars, k_{T2} is torsional stiffness between parts 7 and 8 and parts 8 and 9 of the discretized sheet metal packet and $k_{T1,0}$ and $k_{T2,0}$ are their initial estimated values. It holds that $\mathbf{K}_{C,D} = \mathbf{K}_{C,D}(p_1, p_2)$. The last optimization parameter p_3 is the ratio

$$p_3 = \frac{l}{l_0}, \quad (20)$$

where l_0 is initial end bar length and l is actual end bar length between the rings and laminated armature. The change of this length causes the change of the end bar stiffnesses

$$\begin{aligned} k_\xi(p_3) &= \frac{k_{\xi 0}}{p_3}, & k_\eta(p_3) &= \frac{k_{\eta 0}}{p_3^2}, & k_\zeta(p_3) &= \frac{k_{\zeta 0}}{p_3^3}, \\ k_{\xi\xi}(p_3) &= \frac{k_{\xi\xi 0}}{p_3}, & k_{\eta\eta}(p_3) &= \frac{k_{\eta\eta 0}}{p_3}, & k_{\zeta\zeta}(p_3) &= \frac{k_{\zeta\zeta 0}}{p_3}, \end{aligned} \quad (21)$$

according to the basic elasticity theory. This dependency can be generally written for coupling stiffness matrix as $\mathbf{K}_V = \mathbf{K}_V(p_3)$.

Parameter tuning is considered as an optimization process. Initial model parameter values are defined by estimated values of the stiffnesses which corresponds to the relative optimization parameter vector $\mathbf{p} = [1, 1, 1]^T$. The objective function is chosen in the form

$$\psi(\mathbf{p}) = \sum_{i=1}^3 \left(1 - \frac{\hat{f}_i}{f_i(\mathbf{p})} \right)^2, \quad (22)$$

ν	$f_{\nu 0}$ [Hz]	f_{ν} [Hz]	eigenmode character
1	0	0	rigid body mode
2	96.0	96.0	axial, bearings
3	111.9	111.9	shaft bending
4	115.9	115.9	shaft bending
5	454.8	454.3	shaft bending
6	495.7	494.9	shaft bending
7	740.8	739.7	shaft bending
8	812.4	795.0	torsion
9	826.6	824.6	shaft bending
10	957.9	957.4	shaft bending
14	1476.2	1284.0	torsion
15	1692.3	1429.2	rings and shaft bending
16	1692.3	1429.2	rings and shaft bending
19	1885.5	1563.0	torsion

Tab.1: Eigenfrequencies of the rotor model before ($f_{\nu 0}$) and after (f_{ν}) parameter tuning

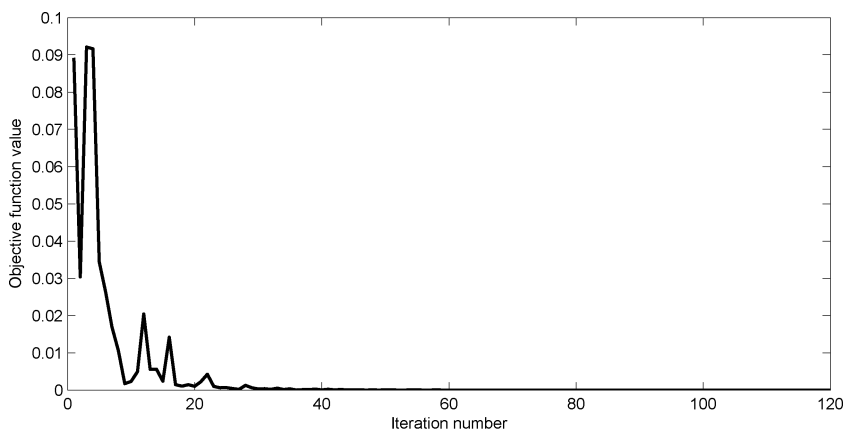


Fig.3: Value of the objective function in the course of optimization process.

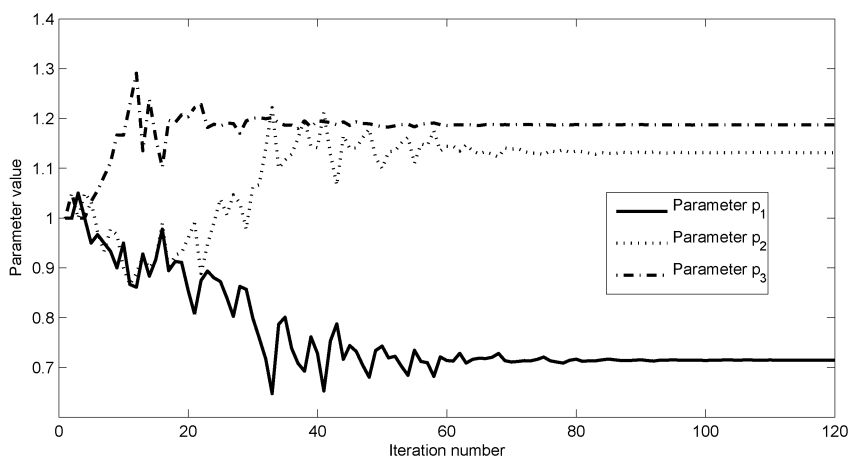


Fig.4: Values of the optimization parameters in the course of optimization process..

where $f_i(\mathbf{p})$ are actual values of eigenfrequencies corresponding to the first three eigenmodes with dominant torsional deformation and \hat{f}_i are measured eigenfrequencies (795 Hz, 1284 Hz and 1563 Hz) corresponding to these eigenmodes (see [4]). Chosen calculated eigenfrequencies of the rotor model before and after the parameter tuning are in Table 1. The dependancies of the objective function value and values of the optimization parameters in the course of optimization process are shown in Figures 3 and 4.

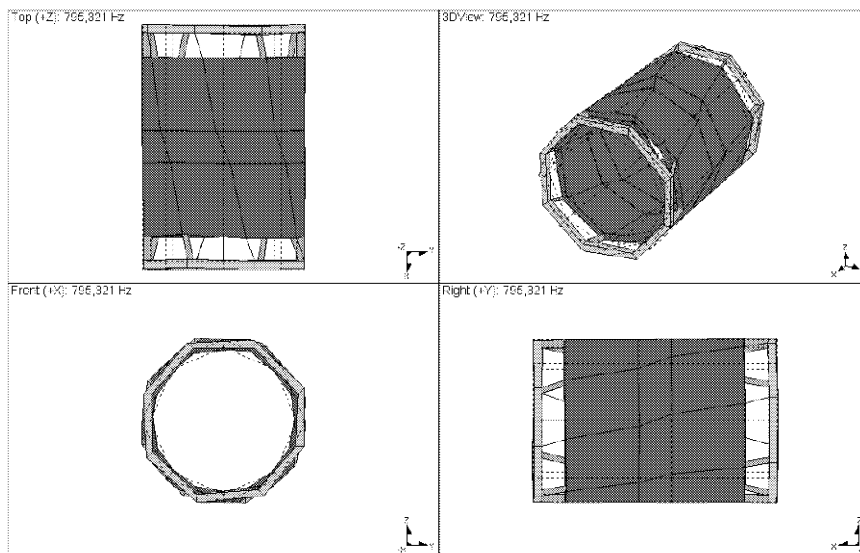


Fig.5: Measured eigenmode characterized by dominant torsional deformation with eigenfrequency 795 Hz (taken from [4])

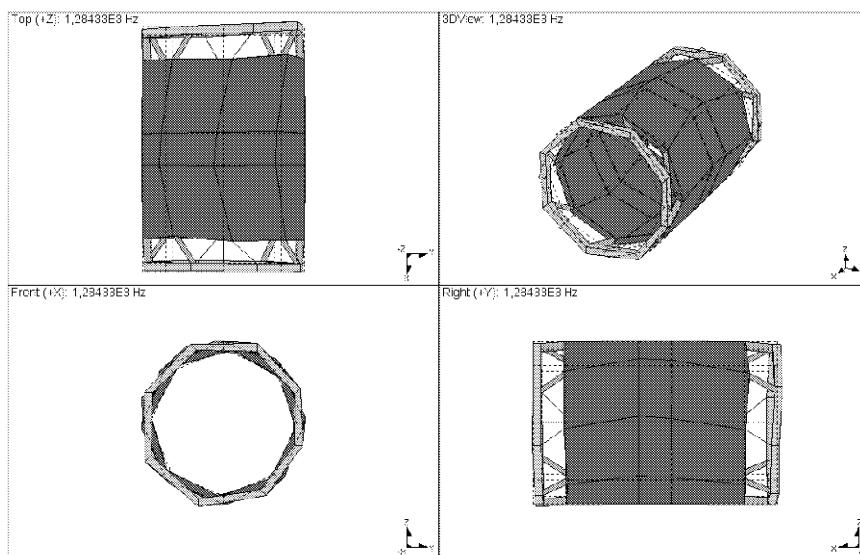


Fig.6: Measured eigenmode characterized by dominant torsional deformation with eigenfrequency 1284 Hz (taken from [4])

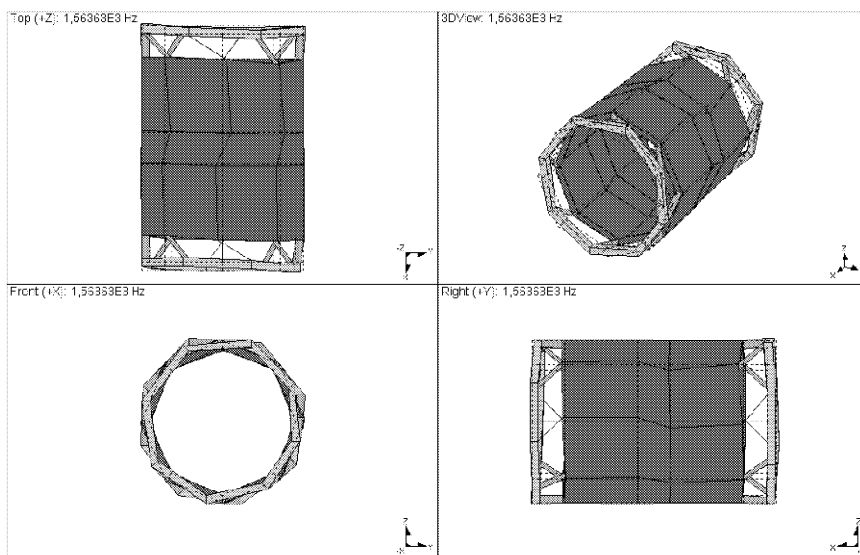


Fig.7: Measured eigenmode characterized by dominant torsional deformation with eigenfrequency 1563 Hz (taken from [4])

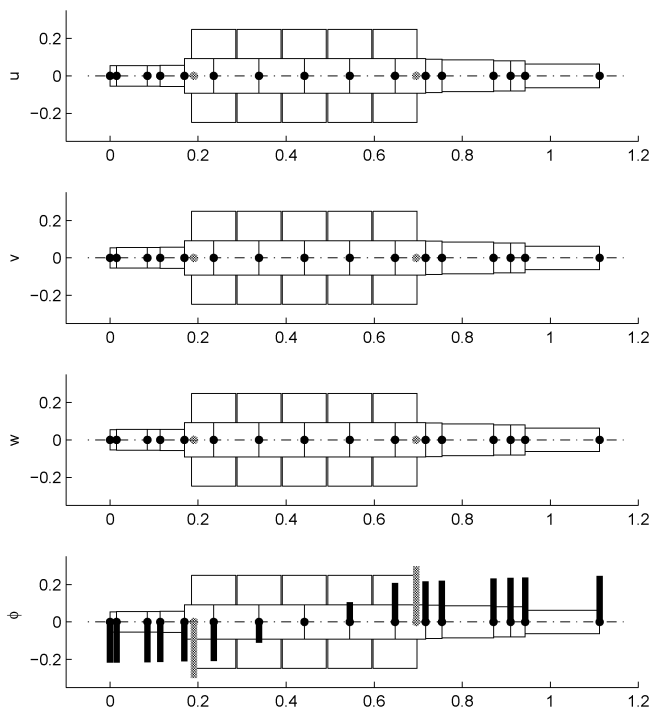


Fig.8: Eigenmode characterized by dominant torsional deformation and by frequency 795 Hz calculated by means of tuned basic dynamic model

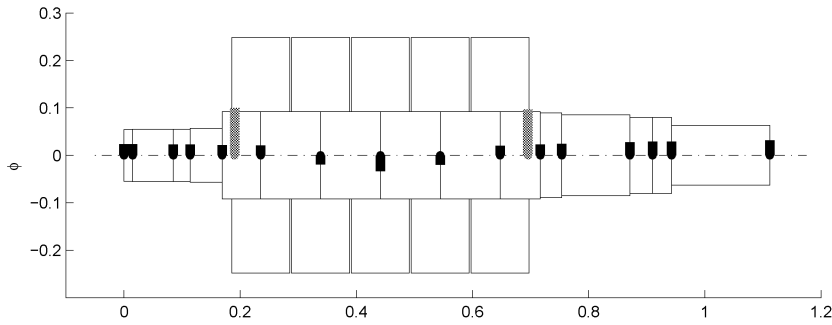


Fig.9: Eigenmode characterized by dominant torsional deformation and by frequency 1284 Hz calculated by means of tuned basic dynamic model

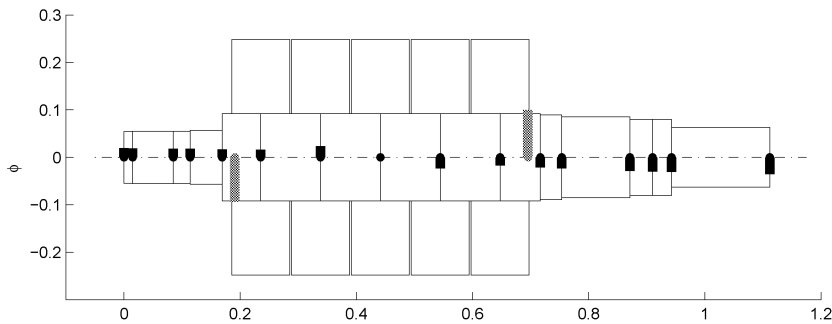


Fig.10: Eigenmode characterized by dominant torsional deformation and by frequency 1563 Hz calculated by means of tuned basic dynamic model

For the illustration chosen measured eigenmodes are shown in Figures 5 to 7. Calculated eigenmodes corresponding to the measured modes are pointed out in Figures 8 to 10. Black nodes correspond to the shaft and grey nodes correspond to the rings. Figure 8 contains also chosen coordinates (see Figure 2) of the eigenvector for the comparison of torsional and translational displacement values. It is clear that the dominant deformation of this eigenmode is only torsional. Translational displacements were omitted in Figures 9 and 10.

4. Conclusion

This paper presents the basic dynamical model of the rotor of the squirrel cage electromotor. The model is characterized by the rigid end and shrink rings and therefore it is suitable rather for low-frequency analysis, where bending and torsional behaviour of the shaft is more dominant. The created computational model can be used for many types of dynamical analyses. The most important ones are modal analysis, steady-state response analysis and non-stationary time integration of motion equations. The excitation can be defined mainly on the basis of electromagnetic field calculation. Future work will be aimed at these analyses and successive output for stress and fatigue investigation. The model can be improved by means of flexible end rings that are discretized by solid finite elements. The basic dynamical model of the rotor can be further used for the component optimization and as a part of more complex drive systems e.g. in rail vehicle dynamics.

Acknowledgement

This work was supported by the research project MSM4977751303 of the Ministry of Education, Youth and Sports of the Czech Republic and by the MPO ČR 2A-2TP1/139 of the Ministry of Industry and Trade of the Czech Republic.

References

- [1] Caruso G. et al.: Torsional eigenfrequency identification of squirrel cage rotors of induction motors, In: International Symposium on Power Electronics, Electrical Drives, Automation and Motion, IEEE, Ischia 2008, pp. 1271–1275
- [2] Hajžman M., Šašek J., Zeman V.: Modelling of flexible rotor vibrations in the rotating coordinate system, In: Modelling, Simulation and Control of Nonlinear Engineering Dynamical Systems. State-of-the-Art, Perspectives and Applications, Springer, 2009, Berlin, pp. 277–288
- [3] Holopainen T.P., Tenhunen A., Arkkio A.: Electromechanical interaction in rotor vibrations of electric machines, In: World Congress on Computational Mechanics 2002, TU Wien, Vienna 2002
- [4] Kroft R.: Modální analýza rotoru pro 109E, Technical report VYZ 1163/2008, ŠKODA VÝZKUM s.r.o., 2008, Plzeň, (in Czech)
- [5] Slavík J., Stejskal V., Zeman V.: Základy dynamiky strojů, CTU Publishing House 1997, Praha, (in Czech)
- [6] Zeman V., Hajžman M.: Modeling of shaft system vibration with gears and rolling-element bearings. In: Colloquium Dynamics of Machines 2005, Institute of Thermomechanics AS ČR, Prague 2005, pp. 163-170

Received in editor's office: March 23, 2010

Approved for publishing: May 27, 2010

Note: This paper is an extended version of the contribution presented at the national colloquium with international participation *Dynamics of Machines 2010* in Prague.